JAST, Vol. 5, No. 1, pp 13–22

JAST
Journal of Aerospace Science and Technology

Compressional Stability Behavior of Composite Plates with Multiple Through-the-Width Delaminations

M. Kharazi[1], H. R. Ovesy[2]

In this paper, the compressive behavior of composite laminates with multiple through-the-width delaminations is investigated analytically. The analytical method is based on the CLPT theory, and its formulation is developed on the basis of the Rayleigh-Ritz approximation technique to analyze the buckling and post-buckling behavior of the delaminated laminates. The method can handle both local buckling of the delaminated sublaminates and global buckling of the whole plate. Also the three-dimensional finite element analysis is performed using ANSYS5.4 general purpose commercial software, and the results are compared with those obtained by the analytical model. The agreement between the results is very good.

INTRODUCTION

Fiber-reinforced composite materials have been increasingly used over the past few decades in a variety of applications in which a fairly high ratio of stiffness/strength to weight is required. However, these materials are prone to a wide range of defects and damages that can cause significant reductions in stiffness and strength. In particular, when the laminated composites are subjected to compressive loads, delamination becomes a constraint in the design process. Various methods have been proposed for the analysis of a plate that contains through-the-width delaminations. Chai *et.al.* have established an analytical one-dimensional model for the analysis of delamination buckling of beam-plate in 1981 [1]. Since then, the delamination buckling of one-dimensional beam-plate has been studied by several researchers. Bottega *et.al.* have analyzed the buckling behavior of circular plates with a circular delamination located in the center of the plate under the assumption of axisymmetric deformation [2]. Shivakumar *et.al.* have studied the buckling behavior of thin elliptical delamination using the Rayleigh-Ritz and finite element method [3]. Anastasiadis *et.al.* have analysed the problem by simulating the contact of the delamination regions through the application of distributed springs of constant stiffness [4]. Davidson has used the Rayeigh-Ritz method to determine the load and strain at which delamination buckling occured for a composite laminate containing a single elliptical shape delamination [5]. Piao has used a consistent shear deformation theory to analyse the beam-plate delamination buckling [6].

Suemasu has studied the buckling behavior of delaminated composite laminates using classical laminate plate theory and first order shear deformation theory [7,8]. Adan *et.al.* have solved the governing differential equation for beams with multiple through the width delaminations to find the buckling load [9]. Wang *et.al.* have used the spring simulation technique to determine the local buckling load of delaminated beams and plates [10]. They have then used the developed spring simulated model to determine the strain energy release rate of delaminated composite plates [11]. Shahwan *et.al.* have used the nonlinear spring distribution between a thin plate which is bonded laterally to a thick plate to analyse the buckling problem [12]. Sleight *et.al.* have compared the results for the buckling loads of debonded sandwich panel under compression obtained using spring distribution between face sheet and core with the corresponding results obtained utilizing FEM and Rayleigh-Ritz methods, each in a separate experiment [13]. The buckling behavior of the

1. *PhD Candidate, Dept. of Aerospace Eng., Amirkabir Univ. of Tech., Tehran, Iran*
2. *Associated Professor, Dept. of Aerospace Eng., Amirkabir Univ. of Tech., Tehran, Iran, Email: ovesy@aut.ac.ir.*

laminated composites with two centrally through-the-width delaminations has been analyzed by Shu [14]. In his study, the classical laminate theory has been employed and the effects of the constraint imposed by the sublaminates to each other and to the base laminate on the buckling behavior of the plate have been investigated. Andrews *et.al.* have formulated a technique utilizing the classical laminated plate theory to study the elastic interaction of the multiple through the width delaminations in laminated plates subject to static out of plane loading while deforming in cylindrical bending [15]. Kharazi *et.al.* have used the spring simulation technique to analyse the buckling of the laminates including bend-twist coupling effects with multiple embedded delaminations [16]. In this study, the minimization of the total potential energy of the system has been used to obtain the buckling load. Kharazi and Ovesy have investigated the compressive behavior of composite laminates, *i.e.* bucking and post-buckling behavior, with through the width delaminations by developing an analytical method based on Rayleigh-Ritz approximation technique [17]. This method can handle both local buckling of the delaminated sublaminate and global buckling of the whole plate. It is noted that in the latter paper (*i.e.* reference [17]) the behaviour of a laminate, which includes only a single delamination, is investigated.

In the current paper, the compressive behavior of composite laminates with multiple through-the-width delaminations is investigated analytically. The analytical method is based on the CLPT theory and its formulation is developed on the basis of the Rayleigh-Ritz approximation technique to analyze the buckling and post-buckling behavior of delaminated laminates. It is the first time in the literature that by employing simple polynomial functions, a method has been able to handle both local buckling of the delaminated sublaminates and global buckling of the whole plate. The latter characteristic of the method is original in that some interesting results are obtained and compared with those achieved by the application of the finite element method. The agreement between the results is very good. It is noted that no contact between the sublaminates is experienced for the examples considered in the paper.

MODELING TECHNIQUE

In this section the analytical model and the applied theory in this study are briefly outlined. The composite plates which are studied in this paper are thin, so that the CLPT is applied in the analytical formulation. As a result of the CLPT assumption [18]:

$$\bar{u}(x,y,z) = u(x,y) - z\frac{\partial w(x,y)}{\partial x}$$

$$\bar{v}(x,y,z) = v(x,y) - z\frac{\partial w(x,y)}{\partial y}$$

$$\bar{w}(x,y,z) = w(x,y) \tag{1}$$

where $\bar{u}$, $\bar{v}$ and $\bar{w}$ are components of displacements at a general point, whilst u, v and w are similar components at the middle surface ($z = 0$). Using Eq. (1) in the Green's expression for in-plane nonlinear strains and neglecting lower order terms in a manner consistent with the usual Von Karman assumption gives the following expressions for strain at a general point [18]:

$$\bar{\epsilon} = \epsilon + z\psi \tag{2a}$$

where [18]

$$\epsilon = \begin{bmatrix} \frac{\partial u}{\partial x} + \frac{1}{2}\left(\frac{\partial w}{\partial x}\right)^2 \\ \frac{\partial v}{\partial y} + \frac{1}{2}\left(\frac{\partial w}{\partial y}\right)^2 \\ \frac{\partial u}{\partial y} + \frac{\partial v}{\partial x} + \frac{\partial w}{\partial x}\frac{\partial w}{\partial y} \end{bmatrix}, \qquad \psi = \begin{bmatrix} -\frac{\partial^2 w}{\partial x^2} \\ -\frac{\partial^2 w}{\partial y^2} \\ -2\frac{\partial^2 w}{\partial x \partial y} \end{bmatrix} \tag{2b}$$

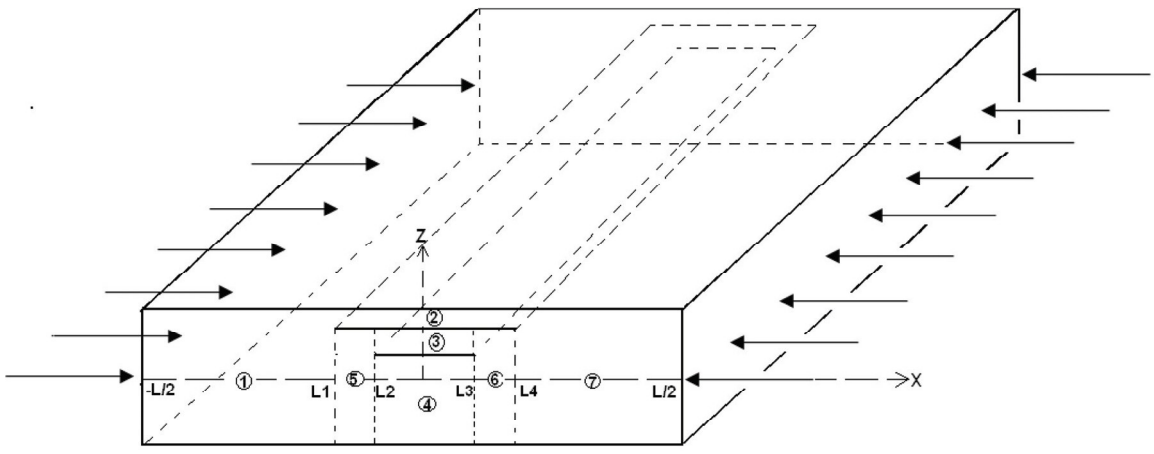

Figure 1. A typical plate with two through the width delaminations.

On the assumption that the plate is in a state of plane stress, the stress-strain relationship at a general point for the plates becomes [18]:

$$\begin{Bmatrix} \bar{\sigma}_x \\ \bar{\sigma}_y \\ \bar{\tau}_{xy} \end{Bmatrix} = \begin{bmatrix} \bar{Q}_{11} & \bar{Q}_{12} & \bar{Q}_{16} \\ \bar{Q}_{12} & \bar{Q}_{22} & \bar{Q}_{26} \\ \bar{Q}_{16} & \bar{Q}_{26} & \bar{Q}_{66} \end{bmatrix} \begin{Bmatrix} \bar{\varepsilon}_x \\ \bar{\varepsilon}_y \\ \bar{\gamma}_{xy} \end{Bmatrix} \tag{3}$$

where $Q_{ij}\,(i,j = 1,2,6)$ are plane stress stiffness coefficients. The constitutive equations for a plate can be obtained through the use of Eqs. (2) and (3) and appropriate integration through the thickness. These equations can be of a very general form which includes general anisotropy and full coupling between in-plane and out-of-plane behavior [18].

$$\begin{Bmatrix} N_x \\ N_y \\ N_{xy} \\ M_x \\ M_y \\ M_{xy} \end{Bmatrix} = \int_{-h/2}^{h/2} z \begin{Bmatrix} \bar{\sigma}_x \\ \bar{\sigma}_y \\ \bar{\tau}_{xy} \\ z\bar{\sigma}_x \\ z\bar{\sigma}_y \\ z\bar{\tau}_{xy} \end{Bmatrix} dz = \begin{bmatrix} [\mathrm{A}] & [\mathrm{B}] \\ [\mathrm{B}] & [\mathrm{D}] \end{bmatrix} \begin{Bmatrix} \{\epsilon\} \\ \{\psi\} \end{Bmatrix} \tag{4}$$

In the above equation N_x, N_y and N_{xy} are the membrane direct and shearing stress resultants per unit length and M_x, M_y and M_{xy} are the bending and twisting stress couples per unit length. The plate stiffness coefficients are defined as [18]:

$$(A_{ij}, B_{ij}, D_{ij}) = \int_{-h}^{h} Q_{ij}(1, z, z^2)dz \qquad (i,j = 1,2,6) \tag{5}$$

The composite plates which are studied in this paper are thin and specially orthotropic and contain through the width delaminations. Because of the symmetry condition about the mid surface of the subject laminates, the in plane and out of plane coupling stiffness coefficients (B_{ij}) are zero. Besides, the plates are subjected to uniform end shortening ϵ at their loaded ends while the unloaded edges are free of any constraint and loadings. As a result, the cylindrical bending assumption is kept valid throughout the analysis. The introduction of the cylindrical bending assumption into Eq. (2) will lead to:

$$\epsilon_x = \left\{ \frac{\partial u}{\partial x} + \frac{1}{2}\left(\frac{\partial w}{\partial x}\right)^2 \right\}$$

$$\psi_x = \left\{ -\frac{\partial^2 w}{\partial x^2} \right\} \tag{6}$$

The strain energy per unit volume is $\frac{1}{2}\bar{\sigma}^T\bar{\epsilon}$. Using Eqs. (6) and (3) to form the strain energy and integrating through the thickness with respect to z gives an expression for the strain energy, which can be put into the form:

$$U = \frac{1}{2}b\int_{-\frac{L}{2}}^{\frac{L}{2}} \left\{A_{11}(\epsilon_{xl})^2 + D_{11}(\psi_x)^2\right\} dx$$

$$+ \frac{1}{2}b\int_{-\frac{L}{2}}^{\frac{L}{2}} \left\{2A_{11}\epsilon_{xnl}\epsilon_{xl} + A_{11}(\epsilon_{xnl})^2\right\} dx \tag{7}$$

where L and b are the length and the width of the laminate respectively, and

$$\epsilon_{xl} = \frac{\partial u}{\partial x}, \qquad \epsilon_{xnl} = \frac{1}{2}\left(\frac{\partial w}{\partial x}\right)^2 \tag{8}$$

In the expression for U there are three contributions that depend upon quadratic, cubic and quartic functions of the displacements. The concern here is with the response of a plate structure to a progressive uniform end shortening ϵ, thus the external force does not exist in the current problem. As a result, the total potential energy is simply equal to the strain energy, *i.e.*

$$\Pi = U \tag{9}$$

Solution to the nonlinear problem is sought through the application of the principle of Minimum Potential Energy. This of course, requires the assumption of a displacement field to represent the variation of u, v and w over the middle surface. Obviously, in a delaminated plate, which is divided into 7 regions as depicted in Figure 1, it is necessary to consider different displacement fields for each separate region. The requirement of the continuity condition is then fulfilled at the boundaries.

The strains in each region can be written as follows:

$$\epsilon_{xl}^{(i)} = \frac{\partial u^{(i)}}{\partial x}, \qquad \epsilon_{xnl}^{(i)} = \frac{1}{2}\left(\frac{\partial w^{(i)}}{\partial x}\right)^2$$

$$\psi_x^{(i)} = -(\frac{\partial^2 w^{(i)}}{\partial x^2}), \qquad i = 1,2,3,4,5,6,7 \tag{10}$$

where $w^{(i)}$ and $u^{(i)}$ are the out of plane and in plane displacement of each region respectively.

The total potential energy of the laminate which is the sum of the strain energies of each region is written as follows:

$$U = \frac{1}{2}b\int_{-\frac{L}{2}}^{L_1} \left\{A_{11}^{(1)}(\epsilon_{xl}^{(1)})^2 + D_{11}^{(1)}(\psi_x^{(1)})^2\right\} dx$$

$$+ \frac{1}{2}b\int_{-\frac{L}{2}}^{L_1} \left\{2A_{11}^{(1)}(\epsilon_{xnl}^{(1)})(\epsilon_{xl}^{(1)}) + A_{11}^{(1)}(\epsilon_{xnl}^{(1)})^2\right\} dx$$

$$
\begin{aligned}
&+\frac{1}{2}b\int_{L_1}^{L_4}\left\{A_{11}^{(2)}(\epsilon_{xl}^{(2)})^2+D_{11}^{(2)}(\psi_x^{(2)})^2\right\}dx\\
&+\frac{1}{2}b\int_{L_1}^{L_4}\left\{2A_{11}^{(2)}(\epsilon_{xnl}^{(2)})(\epsilon_{xl}^{(2)})+A_{11}^{(2)}(\epsilon_{xnl}^{(2)})^2\right\}dx\\
&+\frac{1}{2}b\int_{L_2}^{L_3}\left\{A_{11}^{(3)}(\epsilon_{xl}^{(3)})^2+D_{11}^{(3)}(\psi_x^{(3)})^2\right\}dx\\
&+\frac{1}{2}b\int_{L_2}^{L_3}\left\{2A_{11}^{(3)}(\epsilon_{xnl}^{(3)})(\epsilon_{xl}^{(3)})+A_{11}^{(3)}(\epsilon_{xnl}^{(3)})^2\right\}dx\\
&+\frac{1}{2}b\int_{L_2}^{L_3}\left\{A_{11}^{(4)}(\epsilon_{xl}^{(4)})^2+D_{11}^{(4)}(\psi_x^{(4)})^2\right\}dx\\
&+\frac{1}{2}b\int_{L_2}^{L_3}\left\{2A_{11}^{(4)}(\epsilon_{xnl}^{(4)})(\epsilon_{xl}^{(4)})+A_{11}^{(4)}(\epsilon_{xnl}^{(4)})^2\right\}dx\\
&+\frac{1}{2}b\int_{L_1}^{L_2}\left\{A_{11}^{(5)}(\epsilon_{xl}^{(5)})^2+D_{11}^{(5)}(\psi_x^{(5)})^2\right\}dx\\
&+\frac{1}{2}b\int_{L_1}^{L_2}\left\{2A_{11}^{(5)}(\epsilon_{xnl}^{(5)})(\epsilon_{xl}^{(5)})+A_{11}^{(5)}(\epsilon_{xnl}^{(5)})^2\right\}dx\\
&+\frac{1}{2}b\int_{L_3}^{L_4}\left\{A_{11}^{(6)}(\epsilon_{xl}^{(6)})^2+D_{11}^{(6)}(\psi_x^{(6)})^2\right\}dx\\
&+\frac{1}{2}b\int_{L_3}^{L_4}\left\{2A_{11}^{(6)}(\epsilon_{xnl}^{(6)})(\epsilon_{xl}^{(6)})+A_{11}^{(6)}(\epsilon_{xnl}^{(6)})^2\right\}dx\\
&+\frac{1}{2}b\int_{L_4}^{\frac{L}{2}}\left\{A_{11}^{(7)}(\epsilon_{xl}^{(7)})^2+D_{11}^{(7)}(\psi_x^{(7)})^2\right\}dx\\
&+\frac{1}{2}b\int_{L_4}^{\frac{L}{2}}\left\{2A_{11}^{(7)}(\epsilon_{xnl}^{(7)})(\epsilon_{xl}^{(7)})+A_{11}^{(7)}(\epsilon_{xnl}^{(7)})^2\right\}dx \qquad (11)
\end{aligned}
$$

The $A_{11}^{(i)}$ and $D_{11}^{(i)}$ are the stiffness coefficients in each region.

The requirement of the continuity of the displacement in the boundaries is satisfied as follows:

$$
\begin{aligned}
&w^{(1)}\Big|_{x=L1}=w^{(2)}\Big|_{x=L1}=w^{(5)}\Big|_{x=L1}\\
&w^{(5)}\Big|_{x=L2}=w^{(3)}\Big|_{x=L2}=w^{(4)}\Big|_{x=L2}\\
&w^{(6)}\Big|_{x=L3}=w^{(3)}\Big|_{x=L3}=w^{(4)}\Big|_{x=L3}\\
&w^{(7)}\Big|_{x=L4}=w^{(2)}\Big|_{x=L4}=w^{(6)}\Big|_{x=L4}\\
&w_{,x}^{(5)}\Big|_{x=L_2}=w_{,x}^{(3)}\Big|_{x=L_2}=w_{,x}^{(4)}\Big|_{x=L_2}\\
&w_{,x}^{(3)}\Big|_{x=L_3}=w_{,x}^{(4)}\Big|_{x=L_3}=w_{,x}^{(6)}\Big|_{x=L_3}\\
&w_{,x}^{(2)}\Big|_{x=L_4}=w_{,x}^{(6)}\Big|_{x=L_4}=w_{,x}^{(7)}\Big|_{x=L_4}
\end{aligned}
$$

$$
\begin{aligned}
u^{(1)}\Big|_{x=L_1}&=u^{(2)}\Big|_{x=L_1}-h_2\,w_{,x}^{(1)}\Big|_{x=L_1}\\
&=u^{(5)}\Big|_{x=L_1}+h_5\,w_{,x}^{(1)}\Big|_{x=L_1}\\
u^{(1)}\Big|_{x=L_2}&=u^{(3)}\Big|_{x=L_2}-h_3\,w_{,x}^{(1)}\Big|_{x=L_2}\\
&=u^{(4)}\Big|_{x=L_2}-h_4\,w_{,x}^{(1)}\Big|_{x=L_2}\\
&=u^{(5)}\Big|_{x=L_2}-h_5\,w_{,x}^{(1)}\Big|_{x=L_2}\\
u^{(1)}\Big|_{x=L_3}&=u^{(3)}\Big|_{x=L_3}-h_3\,w_{,x}^{(1)}\Big|_{x=L_3}\\
&=u^{(4)}\Big|_{x=L_3}-h_4\,w_{,x}^{(1)}\Big|_{x=L_3}\\
&=u^{(6)}\Big|_{x=L_3}-h_6\,w_{,x}^{(1)}\Big|_{x=L_3}\\
u^{(1)}\Big|_{x=L_4}&=u^{(2)}\Big|_{x=L_4}-h_2\,w_{,x}^{(1)}\Big|_{x=L_4}\\
&=u^{(6)}\Big|_{x=L_4}-h_6\,w_{,x}^{(1)}\Big|_{x=L_4} \qquad (12)
\end{aligned}
$$

where h_2, h_3, h_4, h_5 and h_6 are respectively the distance between the mid-planes of regions 2, 3, 4, 5 and 6 from the mid-plane of region 1 as shown in Figure 2.

The boundary conditions of the plate in the loading ends can be considered either simply supported or clamped. The clamped boundary conditions with regard to the displacement w are:

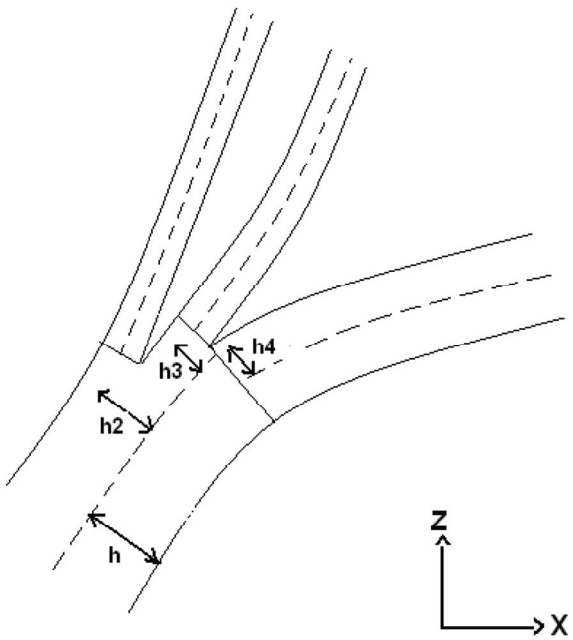

Figure 2. The delamination front.

$$w^{(1)}\Big|_{x=-\frac{L}{2}} = w^{(7)}\Big|_{x=\frac{L}{2}} = 0$$

$$w^{(1)}_{,x}\Big|_{x=-\frac{L}{2}} = w^{(7)}_{,x}\Big|_{x=\frac{L}{2}} = 0 \qquad (13)$$

The functions describing the displacement fields for the divided regions are taken to be polynomials [17]. For clamped boundary condition the assumed out of plane displacement functions are:

$$w^{(1)} = \sum_{m=0}^{M_1} W_m^{(1)}(x+\frac{L}{2})^2(x-\frac{L}{2})^2x^m$$

$$w^{(2)} = \sum_{m=0}^{M_1} W_m^{(1)}(x+\frac{L}{2})^2(x-\frac{L}{2})^2x^m + \sum_{m=0}^{M_2} W_m^{(2)}(x-L_1)^2(x-L_4)^2x^m$$

$$w^{(3)} = \sum_{m=0}^{M_1} W_m^{(1)}(x+\frac{L}{2})^2(x-\frac{L}{2})^2x^m + \sum_{m=0}^{M_3} W_m^{(3)}(x-L_2)^2(x-L_3)^2x^m$$

$$w^{(4)} = \sum_{m=0}^{M_1} W_m^{(1)}(x+\frac{L}{2})^2(x-\frac{L}{2})^2x^m + \sum_{m=0}^{M_4} W_m^{(4)}(x-L_2)^2(x-L_3)^2x^m$$

$$w^{(5)} = \sum_{m=0}^{M_1} W_m^{(1)}(x+\frac{L}{2})^2(x-\frac{L}{2})^2x^m + \sum_{m=0}^{M_5} W_m^{(5)}(x-L_1)^2(x-L_2)^2x^m$$

$$w^{(6)} = \sum_{m=0}^{M_1} W_m^{(1)}(x+\frac{L}{2})^2(x-\frac{L}{2})^2x^m + \sum_{m=0}^{M_6} W_m^{(6)}(x-L_3)^2(x-L_4)^2x^m$$

$$w^{(7)} = \sum_{m=0}^{M_1} W_m^{(1)}(x+\frac{L}{2})^2(x-\frac{L}{2})^2x^m \qquad (14)$$

and the assumed in-plane displacement functions are:

$$u^{(1)} = -x\epsilon + \sum_{m=1}^{N_1} U_m^{(1)}(x+\frac{L}{2})(x-\frac{L}{2})x^m$$

$$u^{(2)} = -x\epsilon + \sum_{m=0}^{N_1} U_m^{(1)}(x+\frac{L}{2})(x-\frac{L}{2})x^m + \sum_{m=0}^{N_2} U_m^{(2)}(x-L_1)^2(x-L_4)^2x^m - h_2\left(\frac{L_1-x}{L_1-L_4}\right)w^{(1)}_{,x}\Big|_{L_4} - h_2\left(\frac{L_4-x}{L_4-L_1}\right)w^{(1)}_{,x}\Big|_{L_1}$$

$$u^{(3)} = -x\epsilon + \sum_{m=0}^{N_1} U_m^{(1)}(x+\frac{L}{2})(x-\frac{L}{2})x^m + \sum_{m=0}^{N_3} U_m^{(3)}(x-L_2)^2(x-L_3)^2x^m - h_3\left(\frac{L_2-x}{L_2-L_3}\right)w^{(1)}_{,x}\Big|_{L_3} - h_3\left(\frac{L_3-x}{L_3-L_2}\right)w^{(1)}_{,x}\Big|_{L_2}$$

$$u^{(4)} = -x\epsilon + \sum_{m=0}^{N_1} U_m^{(1)}(x+\frac{L}{2})(x-\frac{L}{2})x^m + \sum_{m=0}^{N_4} U_m^{(4)}(x-L_2)^2(x-L_3)^2x^m - h_4\left(\frac{L_2-x}{L_2-L_3}\right)w^{(1)}_{,x}\Big|_{L_3} - h_4\left(\frac{L_3-x}{L_3-L_2}\right)w^{(1)}_{,x}\Big|_{L_2}$$

$$u^{(5)} = -x\epsilon + \sum_{m=0}^{N_1} U_m^{(1)}(x+\frac{L}{2})(x-\frac{L}{2})x^m + \sum_{m=0}^{N_5} U_m^{(5)}(x-L_1)^2(x-L_2)^2x^m - h_5\left(\frac{L_1-x}{L_1-L_2}\right)w^{(1)}_{,x}\Big|_{L_2} - h_5\left(\frac{L_2-x}{L_2-L_1}\right)w^{(1)}_{,x}\Big|_{L_1}$$

$$u^{(6)} = -x\epsilon + \sum_{m=0}^{N_1} U_m^{(1)}(x+\frac{L}{2})(x-\frac{L}{2})x^m + \sum_{m=0}^{N_6} U_m^{(6)}(x-L_3)^2(x-L_4)^2x^m - h_6\left(\frac{L_3-x}{L_3-L_4}\right)w^{(1)}_{,x}\Big|_{L_4} - h_6\left(\frac{L_4-x}{L_4-L_3}\right)w^{(1)}_{,x}\Big|_{L_3}$$

$$u^{(7)} = -x\epsilon + \sum_{m=0}^{N_1} U_m^{(1)}(x+\frac{L}{2})(x-\frac{L}{2})x^m \qquad (15)$$

The above expressions are mathematically independent and complete. They also satisfy the boundary conditions and the continuity requirements set forth earlier by Eq's (12-13).

By substituting the assumed displacement functions in the corresponding potential energy expression of each region, the total potential energy of the plate can be evaluated by summation of the potential energies of all regions. In this process, 7 terms are assumed for each series in a given approximation function. It

is noted that the total potential energy of the plate is expressed in terms of a column matrix d which contains all the degrees of freedom as follows:

$$d^T = \left\{ \left\{W_i^{(1)}\right\}^T, \left\{U_i^{(1)}\right\}^T, \left\{W_i^{(2)}\right\}^T, \left\{U_i^{(2)}\right\}^T, \left\{W_i^{(3)}\right\}^T, \left\{U_i^{(3)}\right\}^T, \left\{W_i^{(4)}\right\}^T, \left\{U_i^{(4)}\right\}^T, \left\{W_i^{(5)}\right\}^T, \left\{U_i^{(5)}\right\}^T, \left\{W_i^{(6)}\right\}^T, \left\{U_i^{(6)}\right\}^T \right\} \quad (16)$$

The plate equilibrium equations are obtained by applying the principle of minimum potential energy. That is to say, the partial differential energy with respect to each degree of freedom in turn gives a set of nonlinear equilibrium equations. In the present study the Newton-Raphson iterative procedure is selected for solving the equations. Once the global equilibrium equations are solved and the degrees of freedom are found for a particular prescribed end shortening ϵ, it is possible to calculate the displacements of u and w.

The longitudinal force/load P acting on a laminate at a given end shortening ϵ is determined by integrating the longitudinal mid-plane stresses $\bar{\sigma}$ over the laminate cross-sectional area, *i.e.*

$$\mathrm{P} = -\int_0^b \int_{-h}^{h} \bar{\sigma}_x dz\, dy \quad (17)$$

For the reader's information, the particular end shortening value corresponding to the buckling point, *i.e.* ϵ_{cr}, is found through adopting the procedure outline below.

An arbitrary end shortening ϵ is chosen and used to carry out the post-buckling analysis. If all the degrees of freedom appear to be numerically zero, this will imply that the selected end shortening ϵ has been less than the buckling end shortening. In this case the end shortening is increased by very small increments and the analysis is repeated. This process is continued until non-zero values are obtained for the degrees of freedom when the corresponding end shortening designates the buckling end shortening of the structure ϵ_{cr}. It may be noted that since the size of the increments are successively reduced as the end shortening moves closer to the ϵ_{cr}, it is possible to find the ϵ_{cr} with an accuracy of seven significant digits.

FINITE ELEMENT ANALYSIS

The FEM analysis is performed in order to investigate the validation of the results obtained by the method developed in the current study. The FEM nonlinear buckling analysis is performed employing ANSYS5.4 software, which is a commercially available finite element code. Within ANSYS5.4 software, the buckling analysis is a two-pass analysis. The first pass is a linear static analysis which determines the stresses for a given reference set of loads. The second pass is an eigen-value analysis which provides the results in terms of load factors (eigen-values) and mode shapes (eigen-vectors). Having obtained the mode shapes from an eigen value analysis in the manner described above, they are then used as postulated imperfections in order to perform an iterative nonlinear postbuckling analysis. In this process, the corresponding mode shape is scaled by a small factor (less than 0.0001) and the geometry of the structure is then updated using scaled mode shape as an imperfection. Within nonlinear FEM analysis, the postulation of an imperfection is a necessary step if the postbuckling path after bifurcation point is sought.

The FE Model of the whole composite laminate is generated using 8-node solid elements (solid 46) in order to ensure that a three dimensional finite element analysis is performed. In the bonded regions (*i.e.* undelaminated area), the adjacent elements and corresponding nodes are merged, whilst in the delamination area, the elements are not merged and they are considered separately. Moreover, the mesh is further refined at the discontinuous delamination front in order to preserve the accuracy of the results. Figure 3 shows a typical finite element mesh arrangement adopted in the modeling process for a plate with a through-the-width delamination. It is noted that similar to the developed analytical method the FE analysis is carried out by applying a specified level of uniform end shortening to the loaded ends of the laminates. The application of this end shortening is achieved by enforcing a non-zero displacement constraint in the direction of the end shortening across the laminate at the corresponding loaded ends. This constraint which has the magnitude equal to that of the corresponding end shortening is included in an appropriate set of boundary conditions.

RESULTS AND DISCUSSION

The buckling load of a composite plate with clamped boundary conditions at its loaded ends containing two centrally located through-the-width delamination is given in Figure 4. The lay-up sequence of the

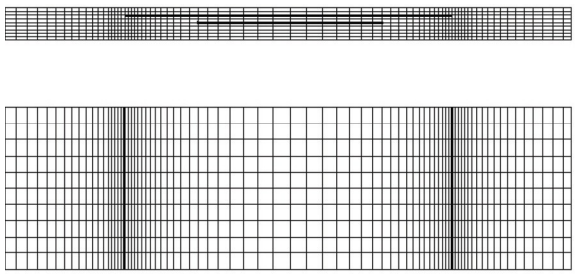

Figure 3. A typical mesh for a laminate with two through-the-width delaminations.

sublaminates and that of the base laminate are [0, 0, 0, 0]. The first delamination is located between the top and the second ply, whilst the second delamination is located between the second and third ply. The results of the finite element analysis, which are obtained by using ANSYS5.4 general purpose commercial software,

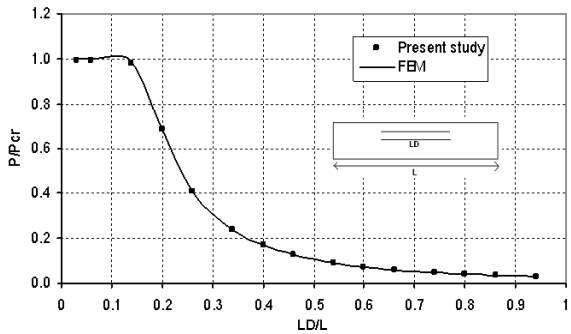

Figure 4. The buckling load of a plate with two centrally located through the width delaminations (LD is the delamination length and P_{cr0} is the buckling load of a plate without any delamination, $L = 300^{mm}$, $2h = 2^{mm}$ (total thickness)).

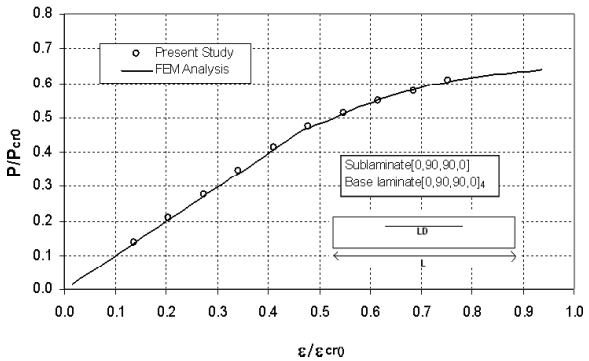

Figure 5. Non-Dimensional load-end Shortening variations for a delaminated clamped plate with a centrally located through the width delamination ($L = 300^{mm}$, $2h = 2^{mm}$, $LD/L = 0.34$ and ϵ_{cr0} is the critical end-shortening corresponding to a plate without any delamination).

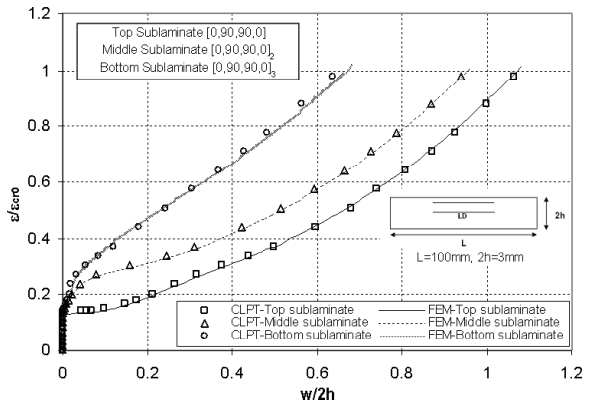

Figure 6. Non-dimensional out of plane displacement variations of a delaminated clamped plate with two centrally located through the width delaminations ($LD/L = 0.58$ and ϵ_{cr0} is the critical end-shortening corresponding to a plate without any delamination).

are also presented for the comparison purpose. A good agreement between the finite element results and those obtained by the present analytical method is clearly seen in the figure.

Figure 5 shows the non-dimensional load-end shortening variations for a clamped-clamped laminate with a centrally located through-the-width delamination. ϵ_{cr0} and P_{cro} are the critical end-shortening and the critical load corresponding to a plate without any delamination. The lay up sequence of the sublaminate and that of the base laminate are [0,90,90,0] and $[0,90,90,0]_4$, respectively. Within the range of end shortening under investigation, a clear post-local-buckling characteristic is demonstrated by the sublaminate, whilst the base laminate remains almost undeformed. The results of the present method are in very good agreement with those obtained by the finite element method of analysis.

Figure 6 shows the variations of the central out of plane displacement ($w/2h$) with the non-dimensional end-shortening for a clamped-clamped plate with two central through-the-width delaminations. ϵ_{cr0} is the critical end-shortening corresponding to a plate without any delamination. The lay up sequence of the top, middle and bottom sublaminates are [0,90,90,0], $[0,90,90,0]_2$ and $[0,90,90,0]_3$ respectively, with the delaminations length 0.58 L. The figure clearly shows that the buckling is initiated in the top sublaminate which is being restrained by the rest of the laminate against further deflection. However, as the end-shortening is increased, the thicker sublaminates start to deflect considerably, and thus their restraint on the top sublaminate is reduced. The latter mixed mode of postbuckling causes a substantial loss in the stiffness of the laminate. It is also seen in the figure that the agreement between the results of the present method and those of FEM are very good.

Figure 7 shows the non-dimensional load-end shortening variations for the same laminate as that discussed in Figure 6. Within the range of end shortening under investigation, a clear post-local-buckling characteristic is demonstrated by the sublaminates. ϵ_{cr0} and P_{cro} are the critical end-shortening and the critical load corresponding to a plate without any delamination respectively. The results of the present method are in good agreement with those obtained by the finite element method of analysis. It can be seen that when the level of applied end shortening reaches the value corresponding to the critical end shortening for a plate without any delamination (*i.e.* when ϵ/ϵ_{cr0} =1.0), the plate's load carrying capacity is less than 40 percent of the critical buckling load of a plate without any delamination. This clearly indicates that the plate has experienced 60 percent of loss in its load carrying capacity due to the presence of delaminations at the aforementioned level of end shortening (*i.e.* at ϵ/ϵ_{cr0}

=1.0). As a result of this investigation, it seems that a proper post-buckling analysis of the delaminated plates similar to that developed in the current study is essential.

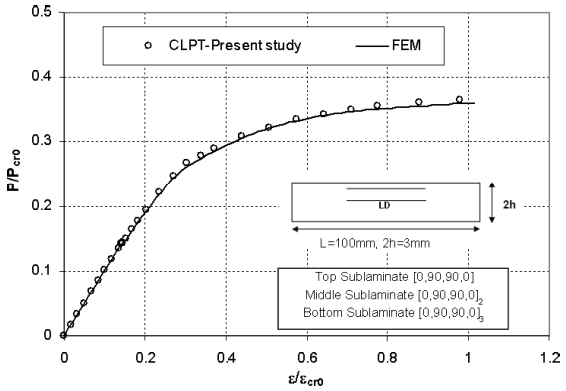

Figure 7. Non-dimensional load-end shortening variations for a delaminated clamped plate with two centrally located through the width delaminations, (LD/L = 0.58), ϵ_{cr0} and P_{cro} are the critical end-shortening and critical load corresponding to a plate without any delamination.

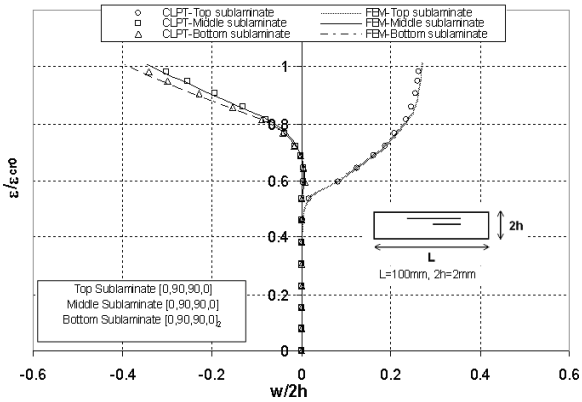

Figure 8. Non-dimensional out of plane displacement variations of a delaminated clamped plate with two through the width delamination (L_1=-20^{mm}, L_2=0, L_3=L_4=20 ^{mm}), ϵ_{cr0} is the critical end-shortening corresponding to a plate without any delamination).

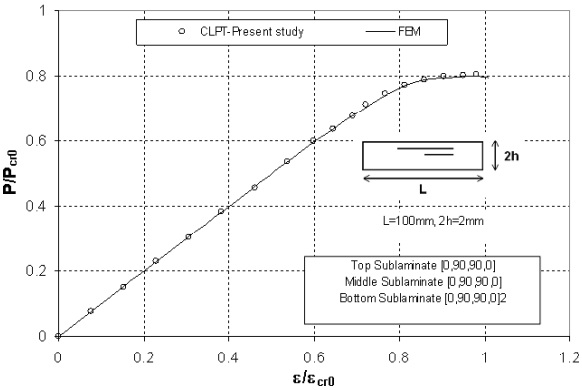

Figure 9. Non-dimensional load-end shortening variations for of a delaminated clamped plate with two through the width delaminations (L_1=-20 ^{mm}, L_2=0, L_3=L_4=20 ^{mm}), ϵ_{cr0} and P_{cro} are the critical end-shortening and critical load corresponding to a plate without any delamination.

Figure 8 shows the variations of the central out of plane displacement of the delaminated sublaminates ($w/2h$) with the non-dimensional end-shortening for a clamped-clamped plate with two through-the-width delaminations. ϵ_{cr0} is the critical end-shortening corresponding to a plate without any delamination. The lay-up sequence of the top, middle and bottom sublaminates are [0,90,90,0], [0,90,90,0] and $[0,90,90,0]_2$ respectively. The laminate length is $L = 100^{mm}$, L_1=-20^{mm}, L_2=0 and L_3=L_4=20^{mm}. The figure clearly shows that the buckling is initiated in the top sublaminate which is being restrained by the rest of the laminate against further deflection. However, as the end-shortening is increased, the thicker sublaminates start to deflect considerably, and thus their restraint on the top sublaminate is reduced. It is also seen in the figure that the agreement between the results of the present method and those of FEM is very good.

Figure 9 shows the non-dimensional load-end shortening variations for the same laminate as that discussed in Figure 8. Within the range of end shortening under investigation, a clear post-local-buckling characteristic is demonstrated by the sublaminates. ϵ_{cr0} and P_{cro} are the critical end-shortening and the critical load corresponding to a plate without any delamination The results of the present method are in very good agreement with those obtained through the finite element method of analysis.

The final investigation is related to the laminate which is essentially similar to the laminate discussed earlier in connection with the results presented in Figures (8-9), except for the fact that in the current investigation the position of the delaminations across the thickness of the laminate is exchanged. That is to say that the shorter delamination is located close to the surface of the laminate. The geometry parameters of the laminate are: $L = 100^{mm}$, $L_1 = 0$, $L_2 = -20^{mm}$ and L_3=L_4=20^{mm}, where ϵ_{cr0} is the critical end-shortening corresponding to a plate without any delamination. The variations of the central out of plane displacement of the delaminated sublaminates ($w/2h$) with the non-dimensional end-shortening are shown in Figure 10. The figure clearly shows the mixed mode of the postbuckling of the laminate. It is also seen in the figure that the agreement between the results of the present method and those of FEM are very good.

Figure 11 shows the non-dimensional load-end shortening variations for the same laminate as that discussed in Figure 10. Within the range of end shortening under investigation, a clear post-local-buckling characteristic is demonstrated by the sublaminates. ϵ_{cr0} and P_{cro} are the critical end-shortening and the critical load corresponding to a plate without any delamination respectively. The results of the present

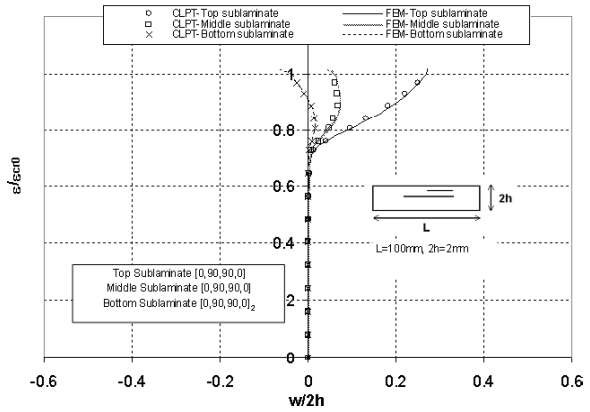

Figure 10. Non-dimensional out of plane displacement variations of a delaminated clamped plate with two through the width delaminations ($L_1 = 0$, $L_2 = -20^{mm}$, $L_3 = L_4 = 20^{mm}$), ϵ_{cr0} is the critical end-shortening corresponding to a plate without any delamination).

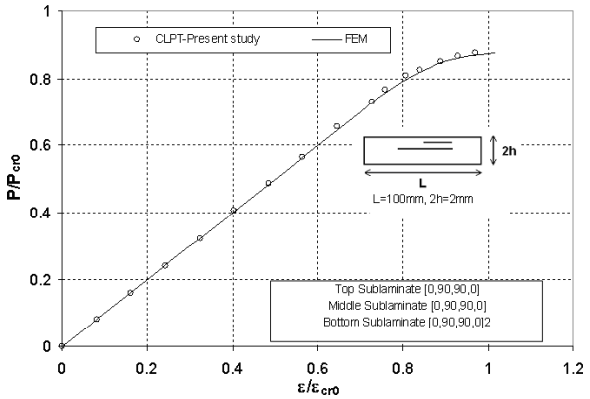

Figure 11. Non-Dimensional Load-End Shortening Variation for of a delaminated clamped plate with two through the width delaminations ($L_1 = 0$, $L_2 = -20^{mm}$, $L_3 = L_4 = 20^{mm}$), ϵ_{cr0} and P_{cro} are the critical end-shortening and critical load corresponding to a plate without any delamination

method are in good agreement with those obtained through the finite element method of analysis.

Moreover, the comparison between the results presented in the last two figures (*i.e.* Figures (10-11)) and the corresponding results presented in Figures 8 and 9 reveals the importance of the kind of analysis carried out in this paper. This is due to the fact that the change in the positions of delaminations has caused a significantly different post-buckling behaviour for the laminates.

CONCLUSION

The compressive behavior of orthotropic composite laminates with multiple through-the-width delaminations is investigated analytically. The method has demonstrated its special capability in analyzing the mixed mode of local buckling of the delaminated sublaminates with the global buckling of the base laminate. It is seen that the buckling loads of the plates with two delaminations are decreased through increasing the delaminations length. It is also seen that the mode of post-buckling and the corresponding load-carrying capacity strongly depends on the delaminations length and depth. The finite element analysis is performed using ANSYS5.4 general purpose commercial software, and the results are compared with those obtained by the analytical model. The agreement between the results is very good.

REFERENCES

1. Chai, H., Babcock, C. D. and Knauss,W. G., "One Dimensional Modeling of Failure in Laminated Plates by Delamination Buckling", *International Journal of Solids and Structures*, **17**, PP 1069-1083(1981).
2. Bottega, W. J. and Maewal, A., "Delamination Buckling and Growth in Laminates", *Journal Applied Mechanics*, **50**, PP 184-189(1983).
3. Shivakumar, K. N. and Withcomb, J. D., "Buckling of Sublaminate in a Quasi Isotropic Composite Laminates", *Journal of Composite Materials*, **19**, PP 2-18(1985).
4. Anastasiadis, J. S. and Simitses, G. J., "Spring Simulated Delamination of Axially Loaded Flat Laminates", *Composite Structures*, **17**, PP 67-85(1991).
5. Davidson, B. D., "Delamination Buckling: Theory and Experiment", *Journal of Composite Materials*, **25**, PP 1351-1378(1991).
6. Piao, C. H., "Shear Deformation Theory of Compressive Delamination Buckling and Growth", *AIAA Journal*, **29**(5), PP 813-819(1991).
7. Suemasu, H., "Compressive Behavior of Fiber Reinforced Composite Plates with a Center Delamination", *Adv. Composite Materials*, **1**(1), PP 23-37(1991).
8. Suemasu, H., "Effects of Multiple Delaminations on Compressive Buckling Behaviors of Composite Panels", *Journal of Composite Materials*, **27**(12), PP 1172-1192(1993).
9. Adan, M., Sheinman, I. and Altus, E., "Buckling of Multiply Delaminated Beams", *Journal of Composite Materials*, **28**(1), PP 77-90(1994).
10. Wang, J. T. S. and Cheng, S.H., "Local Buckling of Delaminated Beams and Plates Using Continuous Analysis", *Journal of Composite Materials*, **29**(10), PP 1374-1402(1995).
11. Wang, J. T. S. and Huang, J. T., "Strain Energy Release Rate of Delaminated Composite Plates Using Continuous Analysis", *Journal of Composites Engineering*, **7**, PP 731-744(1994).
12. Shahwan, K. W. and Wass, A. M., "A Mechanical Model for the Buckling of Unilaterally Constrained Rectangular Plates", *International Journal of Solids and Structures*, **31**(1), PP 75-87(1994).
13. Sleight, D. W. and Wang, J. T., "Buckling Analysis of Debonded Sandwich Panel under Compression", *NACA Technical Memorandum*, (1995).

14. Shu, D., "Buckling of Multiple Delaminated Beams", *International Journal of Solids and Structures*, **25**(13), PP 1451-1465(1998).

15. Andrews, N. G., Massabo, R. and Cox, B. N., "Elastic Interaction of Multiple Delaminations in Plates Subject to Cylindrical Bending", *International Journal of Solids and Structures*, **43**, PP 855-886(2006).

16. Kharazi M, Ovesy H. R., GhannadPour S. A. M., "The Buckling of Laminates Including Bending-Twisting Coupling Effects with Multiple Delaminations Using Spring Simulation", *In Proceedings of the Eighth International Conference on Computational Structures Technology*, Civil-Comp Press, Garan Canaria, Spain, (2006).

17. Kharazi, M. and Ovesy, H. R., "Postbuckling Behavior of Composite Plates with Through-the-Width Delaminations", *Journal of Thin-Walled Structure*, **46**, PP 939-946(2008).

18. Whitney J. M., *Structural Analysis of Laminated Anisotropic Plates*, Technomic Publishing Company, (1987).